Hovi A., Lukeš P., Homolová L., Juola J., Rautiainen M. (2022). Small geographical variability observed in Norway spruce needle spectra across Europe. Silva Fennica vol. 56 no. 2 article id 10683. https://doi.org/10.14214/sf.10683

Supplementary file S1

Table S1.1. Calculation of reflectance and transmittance of the foliage samples from the signals measured by the spectrometer.

The raw data were processed into directional-hemispherical reflectance (R) and transmittance (T) as

$$R = \frac{s_R}{s_{ref,R}} \frac{1}{1 - P_{gap,R}} R_{ref}, \text{ and} \quad (1)$$

$$T = \left(\frac{s_T}{s_{ref,T}} - P_{gap,T} \right) \frac{1}{1 - P_{gap,T}} R_{ref}, \quad (2)$$

where s_R and s_T are the measured raw radiation signals (digital numbers) from the reflectance and transmittance measurements of the sample, $s_{ref,R}$ and $s_{ref,T}$ are the measured raw radiation signals from the white reference measurements for reflectance and transmittance, respectively, R_{ref} is the reflectance of the white reference panel (a calibrated Spectralon with 99% nominal reflectance), and $P_{gap,R}$ and $P_{gap,T}$ are gap fractions in the sample (zero for leaves of broadleaved species).

Table S1.2. Summary of the measurement campaigns of Norway spruce needle spectra that were used in this study.

Campaign	Country	Coordinates	Elevation, above sea level	Date	No. of samples (c0/c1) [1]	Reference(s)	Notes
Šumava 2009	Czech Republic	48°59N 13°33E	1160–1300 m	Jun, 2009	18/22	Unpublished previously	No one-year-old (c1) needles measured: in our analysis, we used spectra of c2 needles as proxy of c1.
Hyytiälä 2012	Finland	61°51'N 24°18'E	130–200 m	Jun 11–25, 2012	10/7	Lukeš et al. 2013	
Bílý Kříž 2016	Czech Republic	49°30'N 18°32'E	760–900 m	Aug 30–Sep 2, 2016	19/20	Homolová et al. 2017; Janoutová et al. 2019	One spectrometer used for reflectance, another for transmittance measurements.
Helsinki 2016	Finland	60°13'N 24°55'E	0–60 m	Jun 14–23, 2016 Jul 26–Aug 1, 2016 Sep 12–13, 2016	18/18	Hovi et al. 2017	Measurements were made three times during the growing season. All data were pooled and treated as one campaign in the analysis.
GEOMON 2017	Czech Republic	Ten sites across the Czech Rep.	480–1070 m	Aug 2–23, 2017	123/124	Lhotáková et al. 2021	
HY-JS-BK 2019–20	Finland	61°51'N 24°18'E	130–200 m	Jul 1–11, 2019	9/9	Hovi et al. 2022	The study sites were Hyytiälä (Finland), Järvselja (Estonia), and Bílý Kříž (Czech Republic).
	Estonia	58°17'N 27°18'E	30–45 m	Jul 2–17, 2020	9/9		
	Czech Republic	49°30'N 18°32'E	760–900 m	Sep 19–21, 2019	9/9		

[1] The numbers represent top-of-canopy needles which were used in our analysis. The symbol c0 refers to current-year and c1 to one-year-old needles.

Publications cited in Table S1.2:

Homolová L, Janoutová R, Lukeš P, Hanuš J, Novotný J, Brovkina O, Fernandez RRL (2017) In situ data supporting remote sensing estimation of spruce forest parameters at the ecosystem station Bílý Kříž. Beskydy 10(1,2): 75–86. https://doi.org/10.11118/beskyd201710010075

Hovi A, Raitio P, Rautiainen M (2017) A spectral analysis of 25 boreal tree species. Silva Fenn 51(4): 7753. https://doi.org/10.14214/sf.7753

Hovi A, Schraik D, Hanuš J, Homolová L, Juola J, Lang M, Lukeš P, Pisek J, Rautiainen M (2022) Assessment of a photon recollision probability based forest reflectance model in European boreal and temperate forests. Remote Sens Environ 269: 112804. https://doi.org/10.1016/j.rse.2021.112804

Janoutová R, Homolová L, Malenovský Z, Hanuš J, Lauret N, Gastellu-Etchegorry J-P (2019) Influence of 3D spruce tree representation on accuracy of airborne and satellite forest reflectance simulated in DART. Forests 10: 292. https://doi.org/10.3390/f10030292

Lukeš P, Stenberg P, Rautiainen M, Mõttus M, Vanhatalo KM (2013) Optical properties of leaves and needles for boreal tree species in Europe. Rem Sens Lett 4(7): 667–676. http://dx.doi.org/10.1080/2150704X.2013.782112.

Lhotáková Z, Kopačková-Strnadová V, Oulehle F, Homolová L, Neuwirthová E, Švik M, Janoutová R, Albrechtová J (2021) Foliage biophysical trait prediction from laboratory spectra in Norway spruce is more affected by needle age than by site soil conditions. Remote Sens 13(3): 391. https://doi.org/10.3390/rs13030391

Table S1.3. Details of the instrumentation and measurement protocols used in the Norway spruce needle spectral measurement campaigns.

Campaign	Integrating sphere	Spectrometer	Carrier thickness [1]	Sample placement	White reference	Method used for measuring gap fraction	Max. storage time, storage conditions [2]
Šumava 2009	ASD RTS-3ZC	ASD FieldSpec3	Not available	one row	Spectralon 99%	Digital scanner	1 day, cool
Hyytiälä 2012	ASD RTS-3ZC	ASD FieldSpec3	0.75 mm	two rows	Spectralon 99%	Digital scanner	1 day, cool
Bílý Kříž 2016	ASD RTS-3ZC	ASD FieldSpec3/4	0.75 mm	majority one row (some two rows)	Spectralon 99%	Digital scanner	1 day, cool
Helsinki 2016	ASD RTS-3ZC	ASD FieldSpec4	1.7 mm	two rows	Spectralon 99%	Digital scanner	1 day, cool
GEOMON 2017	ASD RTS-3ZC	ASD FieldSpec4	0.7 mm	majority one row (some two rows)	Spectralon 99%	Digital scanner	2 days, cool
HY-JS-BK 2019–20	ASD RTS-3ZC	ASD FieldSpec4	0.3 mm	one row	Spectralon 99%	Digital scanner	1 day, cool

[1] Thickness of a single carrier, i.e., the distance from the sample surface to the sample port.

[2] Storage time refers to the time period from cutting a branch of a sample tree until the needles were picked from the branch and measured.

Table S1.4. Calculation of within- and between-site (or within- and between-campaign) coefficients of variation, and site and campaign-specific relative standard errors of mean.

Within- and between-site (or within- and between-campaign) coefficients of variation (CV_{within}, $CV_{between}$) were calculated for each analyzed wavelength (λ) as

$$CV_{within}(\lambda) = \sqrt{\frac{\sum_{i=1}^{m}\left(y_{j,i}(\lambda) - \mu_j(\lambda)\right)^2}{m-1}} \times \frac{100\%}{\mu_j(\lambda)}, \text{ and} \quad (3)$$

$$CV_{between}(\lambda) = \sqrt{\frac{\sum_{j=1}^{n}\left(\mu_j(\lambda) - \mu(\lambda)\right)^2}{n-1}} \times \frac{100\%}{\mu(\lambda)}, \quad (4)$$

where $y_{j,i}(\lambda)$ is the value of the ith spectrum in site (campaign) j, $\mu_j(\lambda)$ is the mean of values in j, $\mu(\lambda)$ is the mean of site(campaign)-specific mean values, m is the number of spectra in j, and n is the number of sites (campaigns).

According to an F-test (one-way analysis of variance), the spruce needle spectra (in campaigns where several samples per one tree were measured) did not significantly differ between sample trees in a site. Therefore, samples in one site (or campaign) were assumed independent from each other, and site and campaign-specific relative standard errors of mean (RSE) were calculated as

$$RSE(\lambda) = \frac{CV_{within}(\lambda)}{\sqrt{m}}. \quad (5)$$

Table S1.5. Variation in albedo, reflectance, and transmittance spectra of Norway spruce top-of-canopy needles within and between measurement campaigns. Range of campaign-specific mean values is given, as well as within- and between-campaign coefficients of variation (CV_{within}, $CV_{between}$) and campaign-specific relative standard error of mean (RSE). See Table S1.4 for definitions of the statistics. Values are given separately for current-year (c0) and one-year-old (c1) needles.

	Blue (490 nm)	Green (560 nm)	Red (665 nm)	Near-infrared (865 nm)
Albedo				
Mean of all campaigns, c0	0.093	0.250	0.090	0.895
Mean of all campaigns, c1	0.086	0.198	0.085	0.835
Campaign-specific mean, c0	0.080–0.105	0.203–0.333	0.074–0.106	0.823–0.958
Campaign-specific mean, c1	0.074–0.097	0.162–0.255	0.068–0.105	0.759–0.903
CV_{within}, c0	12.4–48.2	12.1–30.5	12.1–49.5	2.1–5.3
CV_{within}, c1	14.1–72.1	14.1–37.3	12.2–73.2	4.1–8.8
$CV_{between}$, c0	10.9	17.9	12.8	5.7
$CV_{between}$, c1	10.5	16.0	15.0	6.6
RSE, c0	2.2–11.4	1.6–7.2	2.1–11.7	0.4–1.7
RSE, c1	1.8–17.0	1.6–8.8	1.8–17.3	0.6–3.2
Reflectance				
Mean of all campaigns, c0	0.069	0.165	0.063	0.511
Mean of all campaigns, c1	0.062	0.139	0.059	0.505
Campaign-specific mean, c0	0.062–0.075	0.141–0.210	0.057–0.071	0.458–0.550
Campaign-specific mean, c1	0.055–0.070	0.114–0.185	0.053–0.072	0.452–0.540
CV_{within}, c0	11.5–20.9	10.8–17.9	10.2–17.0	3.1–10.5
CV_{within}, c1	5.5–20.0	9.8–27.7	5.6–24.2	3.6–12.0
$CV_{between}$, c0	9.1	14.4	8.8	7.1
$CV_{between}$, c1	10.3	17.3	12.0	7.8
RSE, c0	1.9–3.6	1.4–4.2	1.5–3.3	0.7–2.9
RSE, c1	1.1–7.0	1.4–8.0	1.1–9.2	0.8–4.5
Transmittance				
Mean of all campaigns, c0	0.025	0.085	0.027	0.384
Mean of all campaigns, c1	0.024	0.059	0.026	0.330
Campaign-specific mean, c0	0.009–0.042	0.053–0.123	0.010–0.042	0.331–0.414
Campaign-specific mean, c1	0.008–0.040	0.044–0.073	0.009–0.040	0.283–0.365
CV_{within}, c0	40.4–146.5	22.9–59.0	32.0–122.3	4.5–10.9
CV_{within}, c1	49.8–183.6	31.2–80.3	41.1–179.0	6.9–15.1
$CV_{between}$, c0	51.9	30.7	47.0	7.8
$CV_{between}$, c1	48.9	23.9	46.5	9.6
RSE, c0	9.0–29.0	3.2–13.9	7.2–27.4	0.7–3.0
RSE, c1	9.6–43.3	4.1–18.9	9.7–42.2	0.9–3.6

Table S1.6. Variation in albedo, reflectance, and transmittance spectra of Norway spruce top-of-canopy needles within and between Hyytiälä, Järvselja, and Bílý Kříž study sites in the HY-JS-BK 2019–20 campaign. Range of site-specific mean values is given, as well as within- and between-site coefficients of variation (CV_{within}, $CV_{between}$) and site-specific relative standard error of mean (RSE). See Table S1.4 for definitions of the statistics. Values are given separately for current-year (c0) and one-year-old (c1) needles.

	Blue (490 nm)	Green (560 nm)	Red (665 nm)	Near-infrared (865 nm)
Albedo				
Mean of all sites, c0	0.105	0.262	0.099	0.905
Mean of all sites, c1	0.097	0.203	0.093	0.850
Site-specific mean, c0	0.099–0.117	0.236–0.281	0.093–0.109	0.895–0.911
Site-specific mean, c1	0.095–0.099	0.182–0.218	0.091–0.096	0.822–0.870
CV_{within}, c0	20.8–22.1	11.0–13.4	20.3–23.9	1.9–3.1
CV_{within}, c1	15.7–28.0	9.2–15.9	17.0–30.3	2.6–3.9
$CV_{between}$, c0	10.1	8.9	8.7	1.0
$CV_{between}$, c1	2.4	9.1	2.8	3.0
RSE, c0	6.9–7.4	3.7–4.5	6.8–8.0	0.6–1.0
RSE, c1	5.2–9.3	3.1–5.3	5.7–10.1	0.9–1.3
Reflectance				
Mean of all sites, c0	0.063	0.160	0.057	0.492
Mean of all sites, c1	0.057	0.131	0.053	0.492
Site-specific mean, c0	0.061–0.067	0.144–0.169	0.057–0.058	0.487–0.496
Site-specific mean, c1	0.056–0.058	0.118–0.137	0.052–0.054	0.478–0.500
CV_{within}, c0	4.2–16.9	4.2–13.2	3.0–15.1	2.1–5.8
CV_{within}, c1	2.9–7.6	4.9–9.2	2.9–7.0	2.6–5.1
$CV_{between}$, c0	4.8	8.4	1.9	0.9
$CV_{between}$, c1	2.2	8.5	1.8	2.5
RSE, c0	1.4–5.6	1.4–4.4	1.0–5.0	0.7–1.9
RSE, c1	1.0–2.5	1.6–3.1	1.0–2.3	0.9–1.7
Transmittance				
Mean of all sites, c0	0.042	0.102	0.042	0.414
Mean of all sites, c1	0.040	0.073	0.040	0.358
Site-specific mean, c0	0.037–0.050	0.091–0.112	0.037–0.051	0.402–0.423
Site-specific mean, c1	0.038–0.041	0.065–0.080	0.038–0.042	0.344–0.372
CV_{within}, c0	44.6–54.5	19.5–23.8	45.8–51.8	3.2–4.7
CV_{within}, c1	39.6–68.0	19.0–41.6	38.6–70.1	5.2–9.8
$CV_{between}$, c0	18.2	10.1	18.0	2.5
$CV_{between}$, c1	4.4	11.0	4.9	3.9
RSE, c0	14.9–18.2	6.5–7.9	15.3–17.3	1.1–1.6
RSE, c1	13.2–22.7	6.3–13.9	12.9–23.4	1.7–3.3

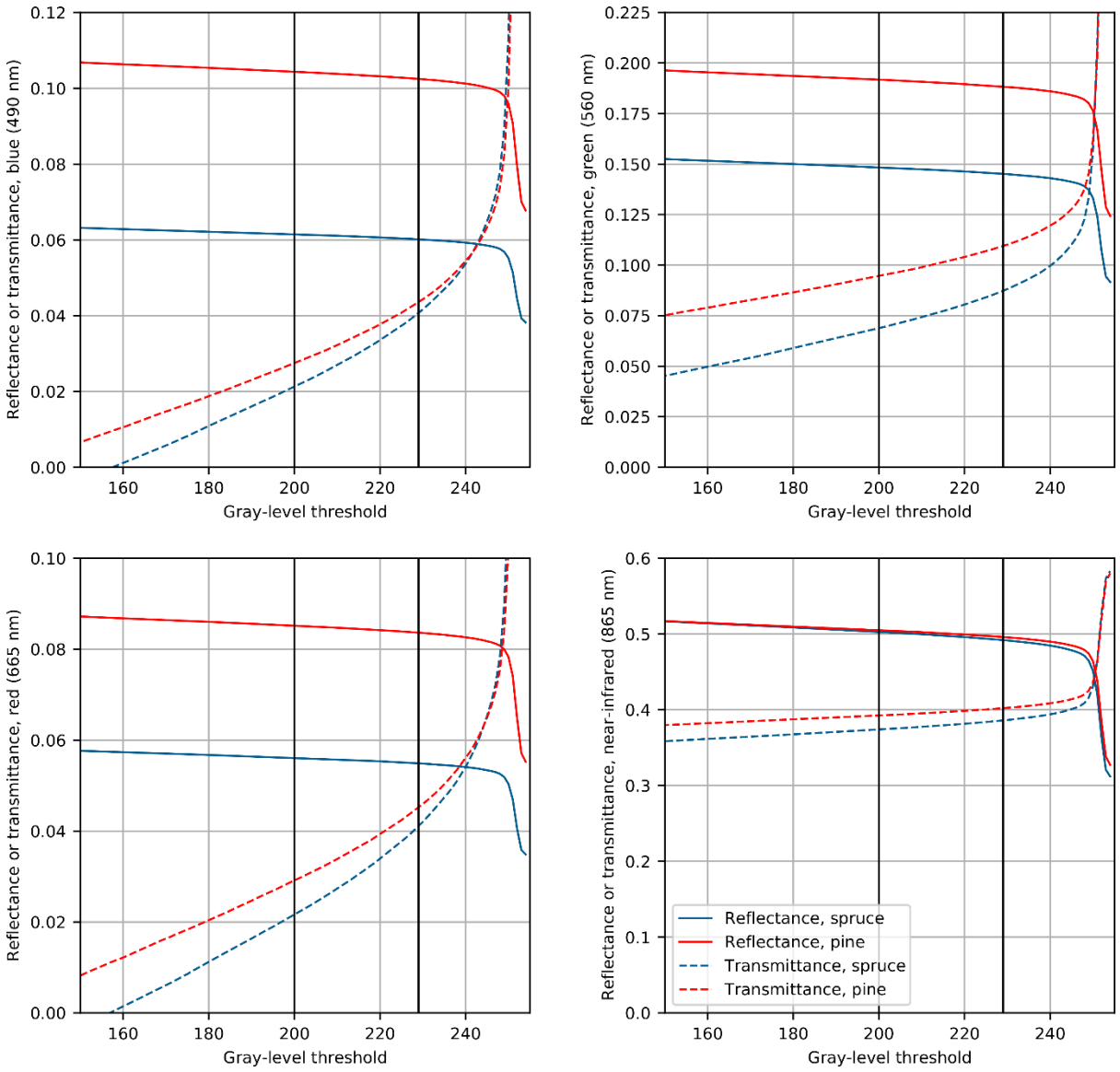

Fig. S1.1. Sensitivity of mean coniferous needle reflectance and transmittance spectra in HY-JS-BK 2019–20 campaign to the gray-level threshold used in determining gap fractions in the needle samples. Both needle age classes (current-year and one-year-old) were pooled together, and only top-of-canopy needles were used here. The vertical black lines show the threshold values (200 for pine, 229 for spruce) used in the analyses of the current study.

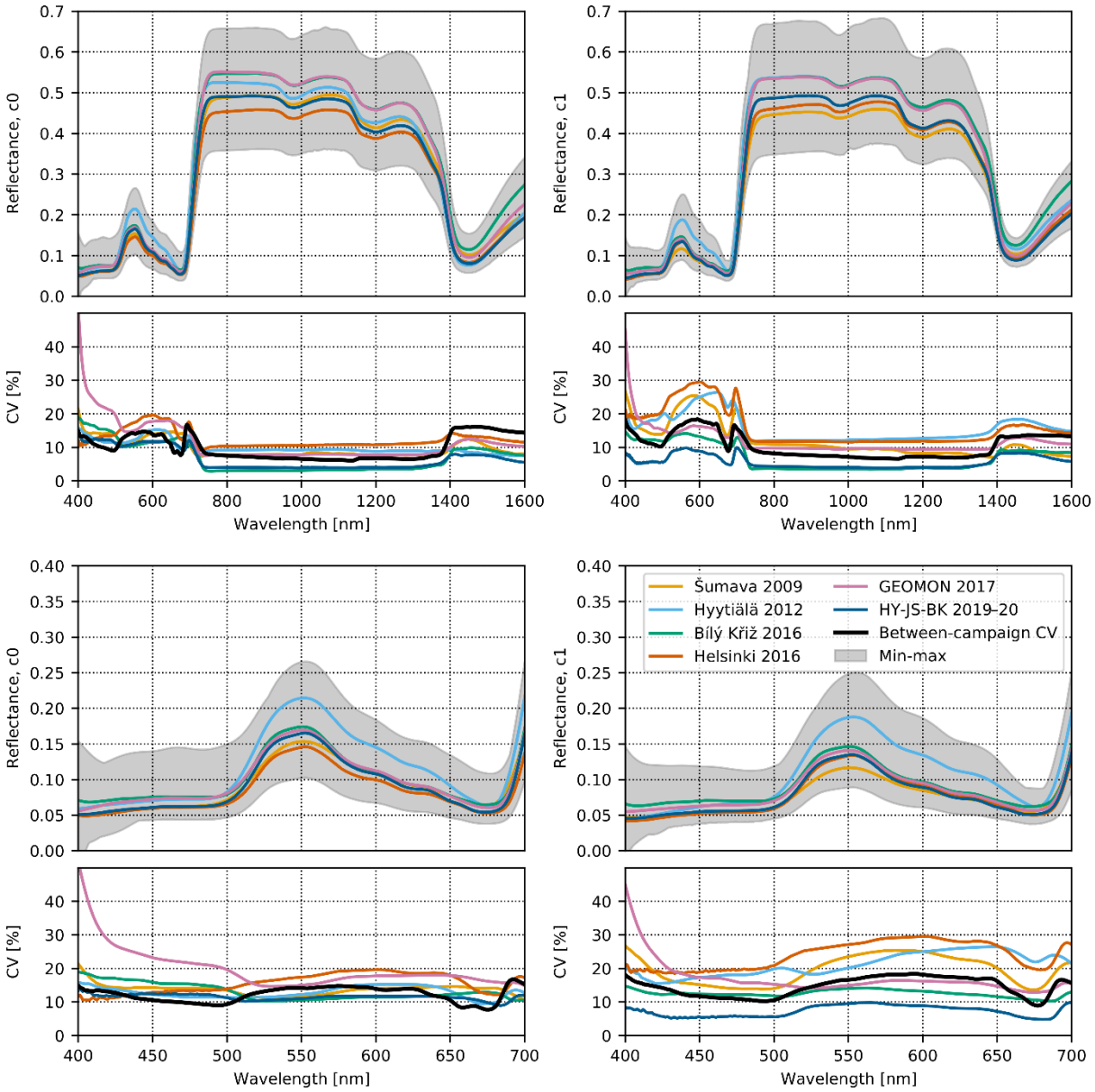

Fig. S1.2. Variation in reflectance spectra of Norway spruce top-of-canopy needles within and between measurement campaigns. CV denotes coefficient of variation. The colored lines show campaign-specific spectra, the thick black line shows between-campaign CV, and the gray area shows min-max of individual spectra among all campaigns. Top row shows full spectra, and bottom row close-ups of the visible wavelength region. The results are shown separately for current-year (c0, left column) and one-year-old (c1, right column) needles.

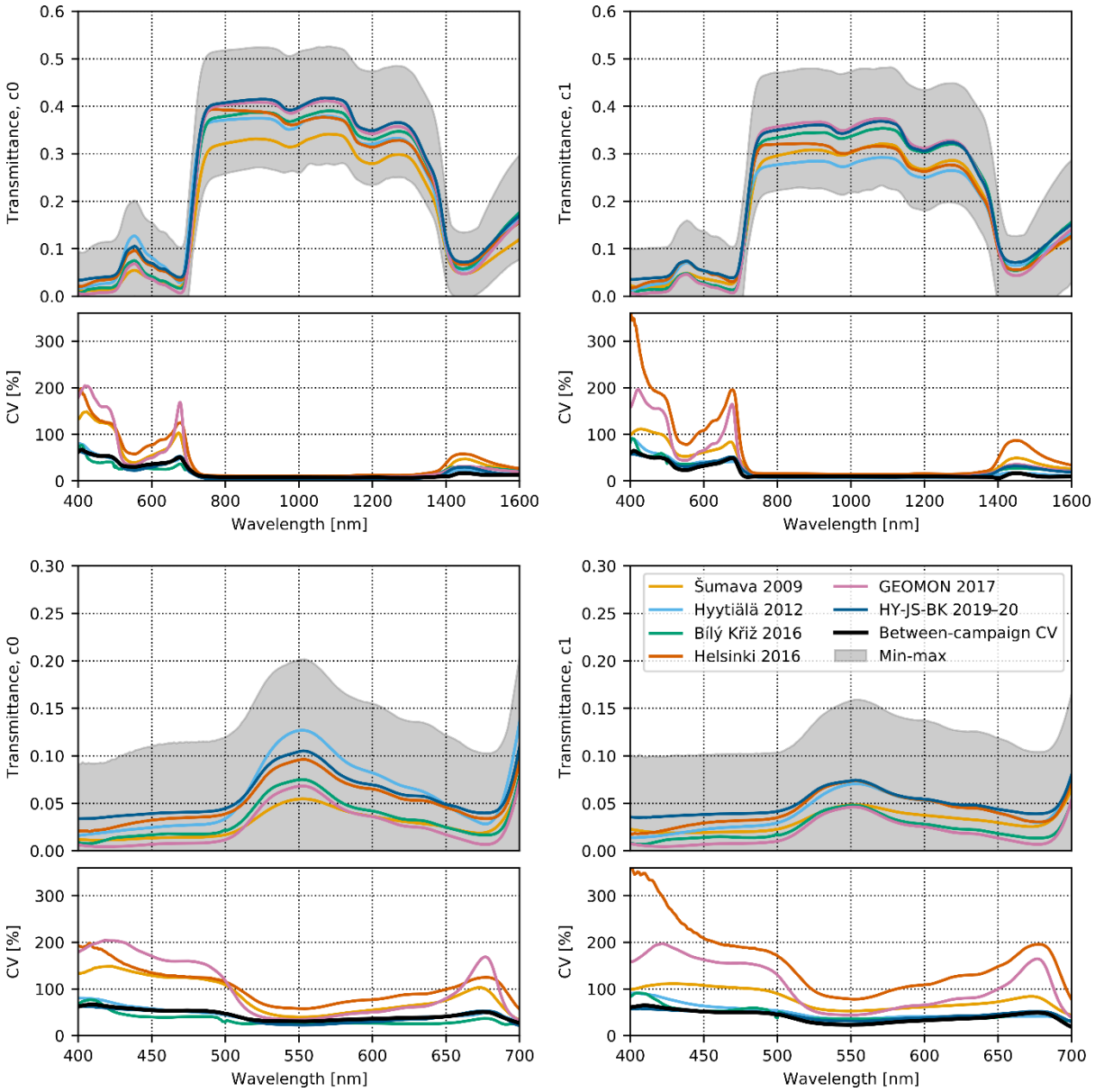

Fig. S1.3. Variation in transmittance spectra of Norway spruce top-of-canopy needles within and between measurement campaigns. CV denotes coefficient of variation. The colored lines show campaign-specific spectra, the thick black line shows between-campaign CV, and the gray area shows min-max of individual spectra among all campaigns. Top row shows full spectra, and bottom row close-ups of the visible wavelength region. The results are shown separately for current-year (c0, left column) and one-year-old (c1, right column) needles.

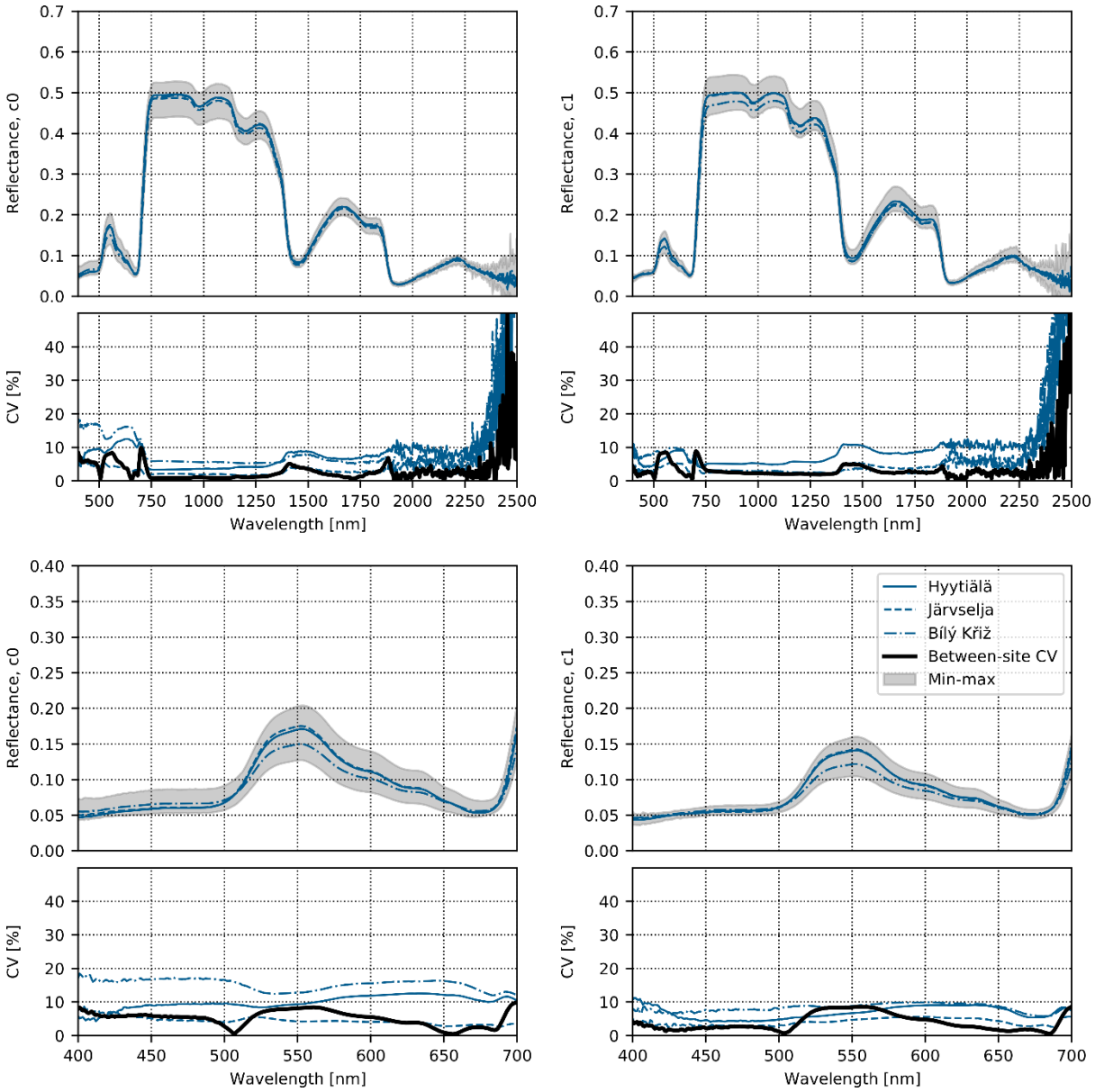

Fig. S1.4. Variation in reflectance spectra of Norway spruce top-of-canopy needles within and between study sites observed in the HY-JS-BK 2019–20 campaign. CV denotes coefficient of variation. The colored lines show site-specific spectra, the thick black line shows between-site CV, and the gray area shows min-max of individual spectra among all sites. Top row shows full spectra, and bottom row close-ups of the visible wavelength region. The results are shown separately for current-year (c0, left column) and one-year-old (c1, right column) needles.

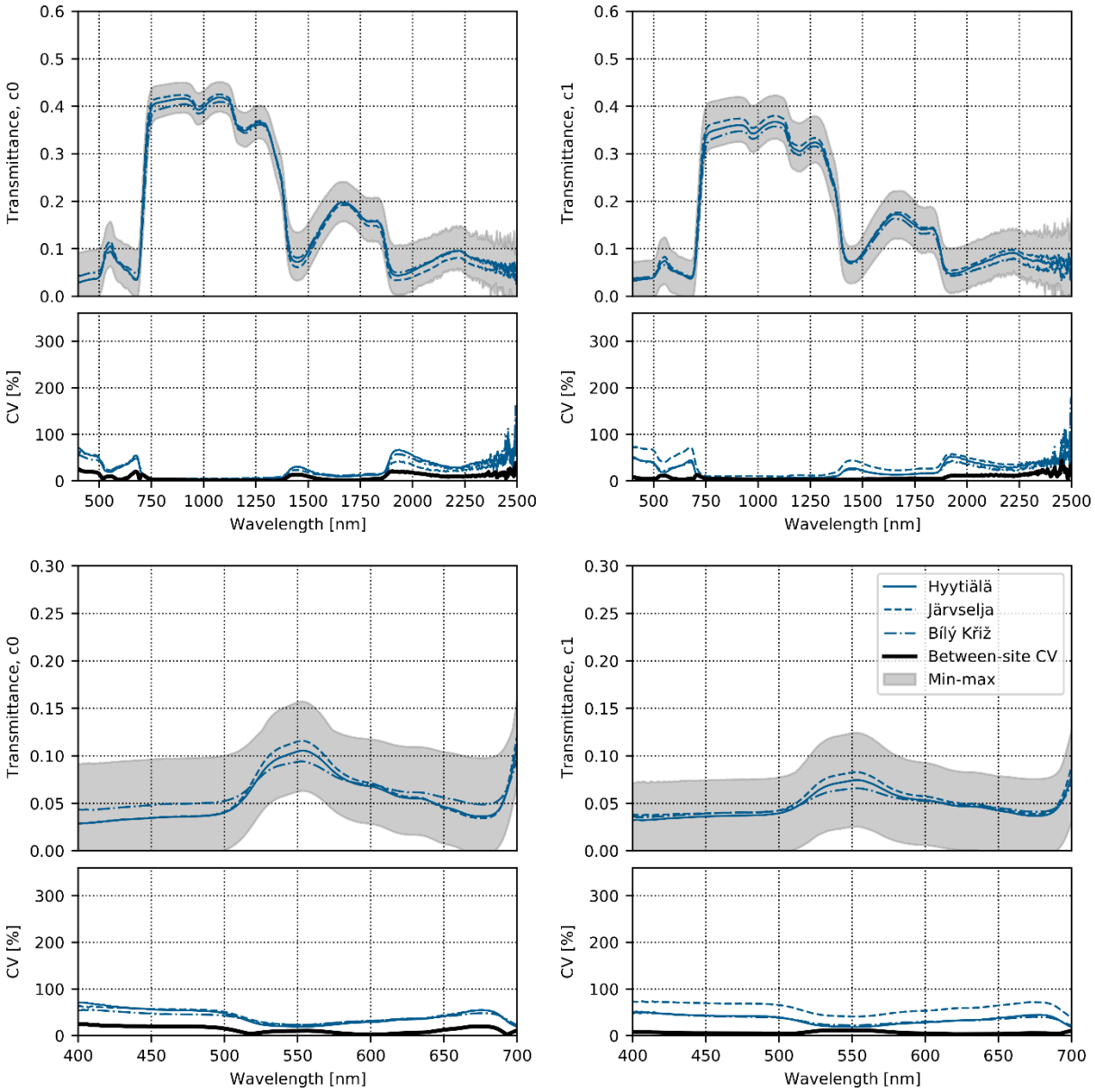

Fig. S1.5. Variation in transmittance spectra of Norway spruce top-of-canopy needles within and between study sites observed in the HY-JS-BK 2019–20 campaign. CV denotes coefficient of variation. The colored lines show site-specific spectra, the thick black line shows between-site CV, and the gray area shows min-max of individual spectra among all sites. Top row shows full spectra, and bottom row close-ups of the visible wavelength region. The results are shown separately for current-year (c0, left column) and one-year-old (c1, right column) needles.

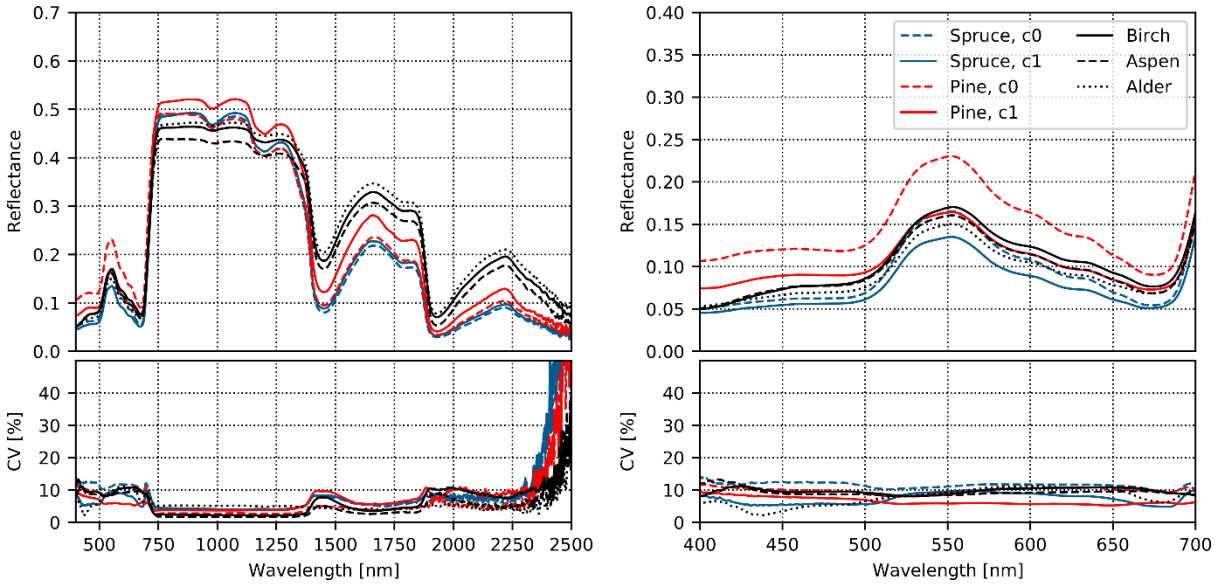

Fig. S1.6. Variation in reflectance spectra of top-of-canopy foliage within- and between tree species. CV denotes coefficient of variation. The right column shows a close-up of the visible wavelength region. The symbol c0 denotes current-year, and c1 one-year-old needles.

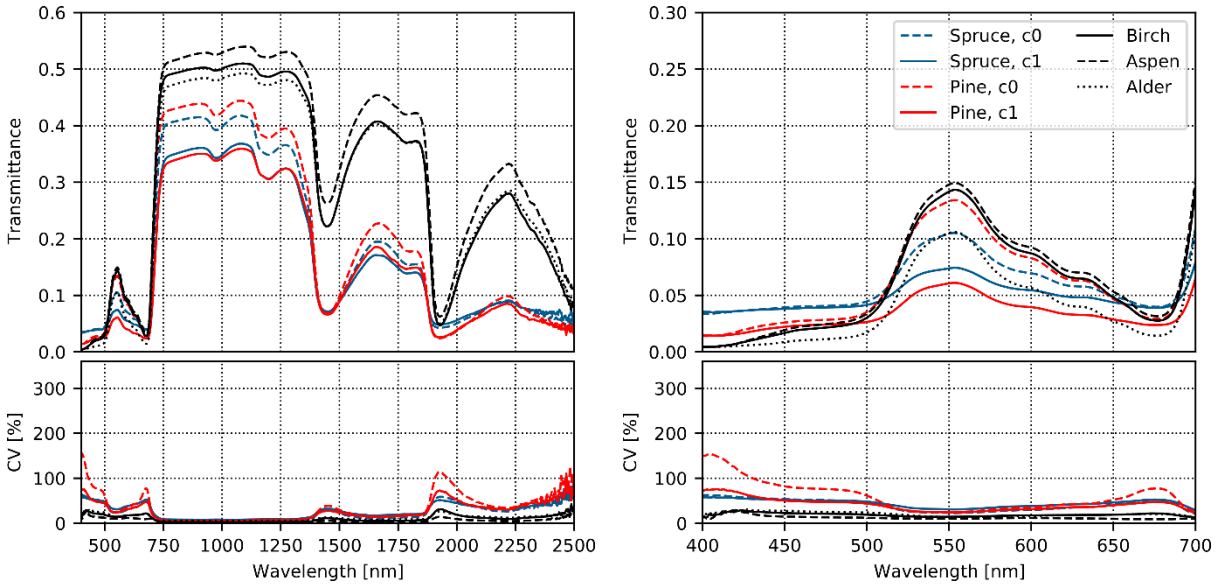

Fig. S1.7. Variation in transmittance spectra of top-of-canopy foliage within- and between tree species. CV denotes coefficient of variation. The right column shows a close-up of the visible wavelength region. The symbol c0 denotes current-year, and c1 one-year-old needles.